Elasticity and Critical Bending Moment of Model Colloidal Aggregates

John P. Pantina and Eric M. Furst*

Department of Chemical Engineering, Colburn Laboratory, University of Delaware, Newark, DE 19716, USA

(Received 19 June 2004; published 7 April 2005)

The bending mechanics of singly bonded colloidal aggregates are measured using laser tweezers. We find that the colloidal bonds are capable of supporting significant torques, providing a direct measurement of the tangential interactions between particles. A critical bending moment marks the limit of linear bending elasticity, past which small-scale rearrangements occur. These mechanical properties underlie the rheology and dynamics of colloidal gels formed by diffusion-limited cluster aggregation, and give critical insight into the contact interactions between Brownian particles.

DOI: 10.1103/PhysRevLett.94.138301 PACS numbers: 82.70.Dd, 82.70.Gg, 83.80.Hj

In the presence of attractive interparticle interactions, colloidal dispersions aggregate to form fractal flocs, where the radius of gyration ξ of an aggregate of k particles with radius a, is given by $\xi = ak^{1/d_f}$. The fractal dimension d_f typically ranges from 1.8 for diffusion-limited cluster aggregation (DLCA) to 2.2 for reaction-limited aggregation (RLA) [1–3]. For strongly flocculating systems, the percolation of this microstructure to form a sample-spanning network marks the transition from a viscous fluid to one that exhibits yield stress and elastic behavior characteristic of a colloidal gel [4,5].

Since colloidal gels are found in a number of technological applications and processes, including high performance coatings, inks, water recovery, and drilling, understanding their structure and rheology is of critical importance. Fundamental to this understanding is the relationship between interparticle interactions, microstructure mechanics, and, ultimately, bulk properties. Using laser tweezers, we have developed methods to directly assemble and measure the mechanical response of single, linear colloidal aggregates. These experiments enable us to independently investigate the mechanical response of the gel microstructure, while circumventing problems commonly encountered when performing bulk rheological measurements of particulate gels, namely, poor reproducibility, dependence on shear history, and limited range of the linear viscoelastic response [4]. Furthermore, the use of simplified aggregate geometries provides insight into the underlying nanoscale interactions between Brownian colloidal particles, where standard theories of colloidal interactions, such as the Derjaguin-Landau-Verwey-Overbeek (DLVO) theory, break down [6].

In this Letter, we report the mechanical response of colloidal aggregates to bending moments as physicochemical conditions are altered. Surprisingly, we find that singly bonded aggregates are capable of supporting torques, reflecting the presence of substantial tangential interactions between particles. Although experimental evidence of tangential forces between colloidal particles has been inferred from observations of particle deposition [7] and differential electrophoresis [8], direct measurement of these forces has been elusive. In previous studies, tangential forces on the order of 0.1 pN have been measured at tens of nanometer separations between particles, whereas the particle interactions studied here support shear forces on the order of 10–100 pN. Furthermore, we characterize two regimes of bending based on the emergence of a critical moment, M_c. For $M < M_c$ the aggregates exhibit a linear elastic deformation, consistent with length-dependent spring models [2]. Above M_c, stress in the aggregate is relaxed via small-scale movement of adjacent particles, demonstrating that even strong gels are capable of exhibiting microstructural rearrangements. The critical bending moment should play an important role in defining the length and time scales of aging processes in gels. Before discussing these results, we briefly review our experimental methods.

Our laser tweezer apparatus is constructed around an inverted microscope (Zeiss Axiovert 200), using a 4 W cw Nd:YAG laser ($\lambda = 1064$ nm, Coherent Compass 1064–400 M) to generate the traps. Positioning of the traps in the focal plane is accomplished by controlling the beam angle at the objective back aperture using a pair of perpendicular acousto-optic deflectors (AOD, AA Opto-electronics AA.DTS.XY-400). The AOD allows us to position the traps with a resolution of 0.2 nm at rates on the order of kilohertz. The beam is focused using a $63\times$ numerical aperture (NA) 1.2 water immersion microscope objective (Zeiss C-Apochromat). The use of a high numerical aperture objective maximizes the gradient force generated by the laser, while a water immersion objective minimizes the effect of spherical aberrations in aqueous samples. The trap rigidity is approximately 40 pN/μm. A more detailed description of the experimental apparatus can be found in [6].

The experiments are conducted using monodisperse, charge stabilized particles of poly(methyl methacrylate) (PMMA, Bangs Laboratory, Inc.) with an average diameter of $2a = 1.47 \pm 0.1$ μm and a measured surface potential of -40 ± 3 mV. Screening of the repulsive double-layer interaction is achieved by suspending the particles in aqueous solutions of $MgCl_2$. As reported elsewhere, linear

aggregates are formed and manipulated far from the sample interface, typically >50 μm [6]. The elasticity of the aggregates is measured using a three-point bending geometry, where the two end particles are held in stationary traps, and a bending moment is applied by translating a trap positioned on the center particle at a velocity of 30 nm/s perpendicular to the aggregate. The force applied to the aggregate, F_{bend}, is measured directly by the displacement of the end particles from their equilibrium positions in the stationary traps. Particle positions are measured with an accuracy of ± 33 nm using a weighted centroid method [9].

Figure 1 shows the shape progression of a typical aggregate in response to a bending moment. The particle positions are in good agreement with the shape expected from a thin rigid rod under similar load conditions

$$y(x) = \frac{-F_{\text{bend}}}{EI}\left(\frac{Lx^2}{4} - \frac{|x^3|}{6}\right), \tag{1}$$

demonstrating that the single particle bonds are capable of supporting torques. In Eq. (1), the flexural rigidity is a product of the Young's modulus E and the area moment of inertia I, and L is the length of the aggregate. Thus, it is possible for classical DLCA structures, where large portions of the microstructure are dominated by single-bond interactions, to support stresses. This contradicts many rheological models of gels, which assume that segments of the network connected by single colloidal bonds exhibit free rotation, and therefore, that multiply bonded structures are necessary [10,11]. Such assumptions have been made based on DLVO interactions between particles, which are centro-symmetric. If particles did undergo free rotations, we would expect the aggregates to respond to the bending moment by forming a trianglelike structure with a pivot point at the center particle. Although our experiments demonstrate that singly bonded colloidal aggregates support significant shear forces, small-scale rearrangements within the aggregates are observed.

Figure 2(a) shows a typical force verses deflection curve for our experiment. When a critical moment M_c is reached,

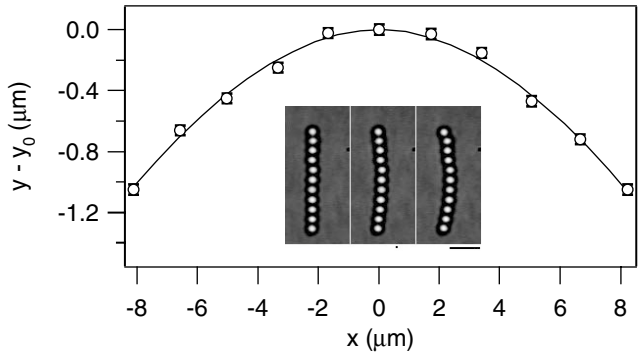

FIG. 1. Bending an 11-particle aggregate in 250 mM $MgCl_2$. The line is a fit of Eq. (1). The scale bar is 5 μm.

a sudden decrease in the supported bending force is observed as δ, the transverse deflection of the center particle relative to the two end points, continues to increase. These mechanics correspond to a short sliding motion of two particles relative to each other (Fig. 2 inset). Over a sample of 25 aggregates, we find that the average length of sliding rearrangements is 32 ± 15 nm, and appears to be independent of salt concentration above approximately 10 mM $MgCl_2$. To find M_c, the position of the particle that underwent a slip x^* is identified. Thus $M_c = F^*_{\text{bend}}(L/2 - |x^* - L/2|)$, where F^*_{bend} is the maximum force measured immediately before the rearrangement [see Fig. 2(a)]. Approximately 90% of the rearrangements occur within 2 particles of the aggregate center, where the bending moment is greatest. Finally, Fig. 2(b) shows M_c as a function of salt concentration. As the salt concentration increases, M_c plateaus to a value of approximately 35 pN μm.

Below the critical bending moment, linear aggregates exhibit an elastic response. The bending rigidity is defined as $\kappa = F_{\text{bend}}/\delta$. Figure 3(a) shows the dependence of κ on contour length s at three concentrations of $MgCl_2$. The bending rigidity increases with ionic strength. Note that the trap compliance limits the maximum rigidity that can be measured. For instance, at 500 mM $MgCl_2$, the elasticity of

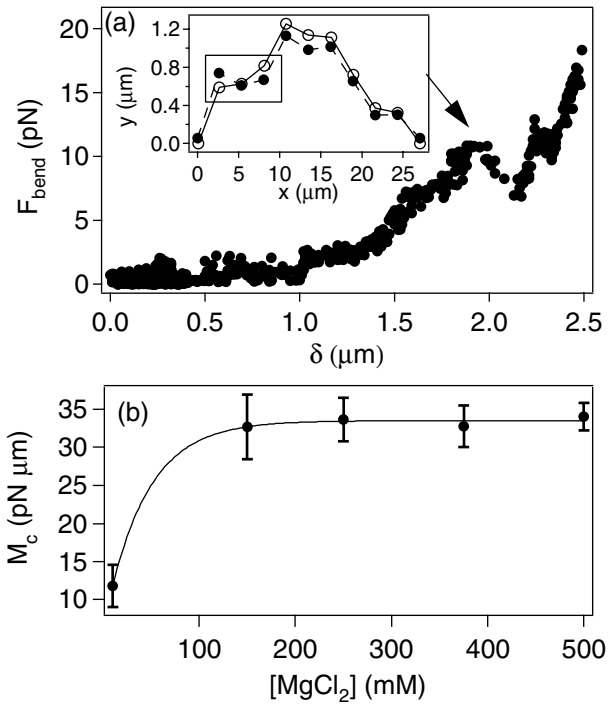

FIG. 2. (a) An example of the tension vs deflection for an 11-particle aggregate in 150 mM $MgCl_2$. Small-scale rearrangements in our experiments (box in inset) correlate with sudden decreases in the resistance to bending and a critical bending force F^*_{bend}. (b) The critical bending moment M_c dependence on $MgCl_2$ concentration.

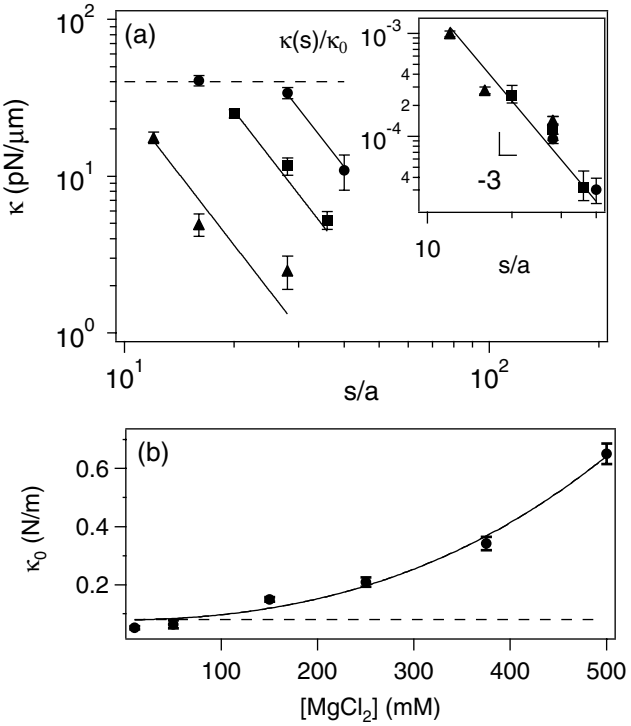

FIG. 3. (a) The measured elasticity vs aggregate length at 50 mM (triangles), 250 mM (squares), and 500 mM (circles) $MgCl_2$. The dashed line is the maximum trap rigidity, 40 pN/μm. The inset shows the scaling of the normalized elasticity $\kappa(s)/\kappa_0 \sim s^{-3}$. (b) The single-bond rigidity increases with salt concentration. The solid line is the fitted κ_0 using JKR theory with $W_{SL}^s = [MgCl_2]^{1.94\pm0.21}$. The dashed line is W_{SL}^0.

9 particle chains is less than the compliance of the laser traps. Measurements made at these conditions, therefore, reflected the compliance of the traps instead of the chain aggregates. As shown in the inset of Fig. 3(a), the measured elasticity of aggregates at all conditions fit a power-law relation with respect to length, with a scaling exponent $\kappa \sim s^{-3}$, as expected from Eq. (1).

Microrheological models of particulate gels generalize Eq. (1) to account for a fractal microstructure. The microstructure elasticity is modeled as $\kappa = \kappa_0(a/s)^{2+d_b}$, where κ_0 is the bond rigidity, and d_b is the bond dimension, the fractal dimension of the stress-bearing backbone structure [2,12]. Computer simulations have shown that $d_b \approx 1.1$ for diffusion-limited clusters [13]. The elastic modulus of the gel can then be estimated as $G \approx \kappa(\xi_c)/\xi_c$, where ξ_c is the radius of gyration of the flocs at the percolation threshold [2], providing a direct connection between the microstructure mechanics and gel rheology. The chain aggregates in the experiments reported here are nearly perfectly straight, i.e., $d_b = 1.0$, and therefore show excellent agreement between the theoretical and observed scaling dependence of $\kappa \sim s^{-3}$. More importantly, the use of linear aggregates enables us to identify and understand the origin of the single-bond rigidity κ_0 and its dependence on physico-chemical conditions, which has been previously unexamined.

By comparing Eq. (1) to the length-dependent spring model discussed above, the single-bond bending rigidity is $\kappa_0 = 3\pi a_c^4 E/4a^3$, where the flexural rigidity in Eq. (1) is $EI = \pi E a_c^4/4$ for a circular contact region with radius a_c. This provides a direct relationship between the bending mechanics and the particle interaction energy, since a_c can be calculated by the theory of particle adhesion due to Johnson, Kendall, and Roberts (JKR) [14]. For equal-sized elastic particles in the absence of an applied normal load, $a_c = (3\pi a^2 W_{SL}/2K)^{1/3}$, where W_{SL} is the adhesion energy per unit area and $K = 2E/3(1-\nu^2)$ is the bulk modulus. The Young's modulus of PMMA is $E = 3100$ MPa and the Poisson ratio is $\nu = 0.4$ [15]. At vanishing salt concentration, W_{SL} is calculated via the Young-Dupré equation $W_{SL}^0 = \gamma_L(1 + \cos\theta_0)$, where $\gamma_L = 72.7$ mN/m and the PMMA-water contact angle is $\theta_0 = 73.7°$ [16]. Note that γ_L is largely insensitive to $MgCl_2$ over the range of concentrations investigated [17]. This leads to a bending rigidity that is in excellent agreement with the values obtained from experiments at low salt concentrations. Using the JKR model, $\kappa_0 = 80$ mN/m, while the experimental value at 10 mM $MgCl_2$ is 64 ± 0.5 mN/m. The corresponding contact area radius is $a_c \approx 40$ nm.

As the concentration of $MgCl_2$ increases, the upward curvature of κ_0 suggests that W_{SL} increases nonlinearly with salt concentration. Expressing the adhesion energy as $W_{SL} = W_{SL}^0 + W_{SL}^s$, where $W_{SL}^s = f([MgCl_2])$ is the additional energy due to the divalent salt, we find that the power-law $W_{SL}^s \sim [MgCl_2]^{1.96\pm0.21}$ fits the data well [cf. Fig. 3(b)]. This increase can be due to several factors, including ion binding and ion-ion correlations. For instance, the Mg^{2+} ions may bind acidic residues on adjacent particles [18]. Force measurements between carboxylated lipid bilayers exhibit increased adhesion forces in the presence of Mg^{2+} and Ca^{2+} [19]. Furthermore, theoretical calculations of double-layer interactions based on the primitive model have shown that divalent ions induce attractive interactions in excess of van der Waals contributions, a phenomena that the Poisson-Boltzmann theory, the basis of DLVO theory, does not capture [20]. Such forces are due to the correlation between ions, and are thought to contribute to the strong adhesion and nonswelling observed for negatively charged clays in solutions of divalent salts [21].

Returning to the critical moment in light of the JKR theory used to model the bending mechanics, the surprising fact that particles do not roll past each other represents the pinning of the solid-solid contact line. This is likely a result of nanoscale surface roughness of the particle interfaces, which explains the insensitivity to salt concentration, in contrast to κ_0 [22]. It is also interesting to note that the length scale of rearrangements between particles for $M > M_c$ is approximately equal to the calculated values of a_c.

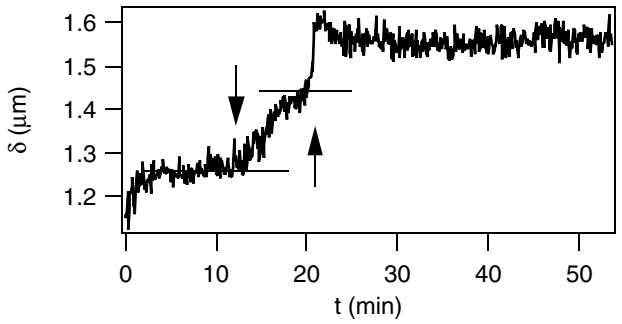

FIG. 4. The response of a 25-particle aggregate in 50 mM $MgCl_2$ to a step stress. An equilibrium deflection is followed by a period of creep, demarcated by the arrows. The end of the creep response is marked by a sudden rearrangement, corresponding to a single-bond slipping.

Finally, the existence of small-scale rearrangements observed above M_c have important implications for the mechanics and dynamics of colloidal gels. In gels, rearrangements will occur on time scales long enough for segments of the gel backbone to overcome the energetic barrier of the critical moment. Such small amplitude dynamics may play a role in the nonlinear behavior of strong colloidal gels, such as the aging and collapse of gels under weak gravitational stresses [23]. To provide an example of spontaneous rearrangements, an aggregate consisting of 25 particles in 50 mM $MgCl_2$ is subjected to a step stress below the critical moment. The resulting response, shown in Fig. 4, initially exhibits elastic deformation, as expected. This is followed by a creeplike behavior starting approximately 10 min after the initial deformation (first arrow), and terminates with a spontaneous relaxation, similar to those that occur at $M > M_c$ (second arrow). Like Fig. 2, a slip rearrangement at one particle bond identified using microscopy correlates with the mechanical relaxation.

In summary, by directly assembling colloidal particles into singly bonded linear aggregates, and applying a bending moment using laser tweezers, we have demonstrated that large tangential interactions between colloidal particles are sufficient for particle bonds to support torques. Furthermore, a critical bending moment has been measured, above which, small-scale particle rearrangements occur. The origin of the tangential interactions is consistent with particle adhesion. Finally, controlling tangential interactions may be important for manipulating the rheology of colloidal gels. Significant tangential forces will strengthen the gel microstructure and result in a higher yield stress and bulk modulus. Conversely, weakened tangential interactions will reduce the compressive yield stress of a gel, which is critical in processes such as water recovery.

This work was supported by the National Science Foundation (CTS-0209936 and CTS-0238589). We acknowledge helpful discussions with K. Miller, J. Crocker, and J. Walz, and the technical assistance of J. Bishop.

*Electronic address: furst@che.udel.edu

[1] D. Weitz and M. Oliveria, Phys. Rev. Lett. **52**, 1433 (1984).
[2] A. Krall and D. Weitz, Phys. Rev. Lett. **80**, 778 (1998).
[3] T. Gisler, R. C. Ball, and D. A. Weitz, Phys. Rev. Lett. **82**, 1064 (1999).
[4] R. G. Larson, *Structure and Rheology of Complex Fluids* (Wiley, New York, 1997).
[5] R. Buscall, I. McGowan, P. Mills, R. F. Steward, D. Sutton, L. White, and G. Yates, J. Non-Newtonian Fluid Mech. **24**, 183 (1987).
[6] J. P. Pantina and E. M. Furst, Langmuir **20**, 3940 (2004).
[7] T. Dabros and T. G. M. van de Ven, Colloid Polym. Sci. **261**, 694 (1983).
[8] D. Velegol, S. Catana, J. Anderson, and S. Garoff, Phys. Rev. Lett. **83**, 1243 (1999).
[9] J. C. Crocker and D. G. Grier, J. Colloid Interface Sci. **179**, 298 (1996).
[10] A. Potanin, R. De Rooij, D. Van den Ende, and J. Mellema, J. Chem. Phys. **102**, 5845 (1995).
[11] A. Potanin and W. Russel, Phys. Rev. E **53**, 3702 (1996).
[12] Y. Kantor and I. Webman, Phys. Rev. Lett. **52**, 1891 (1984).
[13] P. Meakin, Phys. Rev. Lett. **51**, 1119 (1983).
[14] K. L. Johnson, K. Kendall, and A. D. Roberts, Proc. R. Soc. London A **324**, 301 (1971).
[15] G. Schreyer, *Konstruieren mit Kunststoffen* (Carl Hanser, München, 1972).
[16] D. Y. Kwok, A. Leung, C. N. C. Lam, A. Li, R. Wu, and W. Neumann, J. Colloid Interface Sci. **206**, 44 (1998).
[17] N. L. Jarvis and M. A. Scheiman, J. Phys. Chem. **72**, 74 (1968).
[18] T. Ederth and P. M. Claesson, J. Colloid Interface Sci. **229**, 123 (2000).
[19] S. McLaughlin, N. Mulrine, T. Gresalfi, G. Vaio, and A. McLaughlin, J. Gen. Physiol. **77**, 445 (1981).
[20] R. Kjellander, S. Marčelja, R. M. Pashley, and J. P. Quirk, J. Chem. Phys. **92**, 4399 (1990).
[21] R. Kjellander, S. Marčelja, R. M. Pashley, and J. P. Quirk, J. Phys. Chem. **92**, 6489 (1988).
[22] J. M. Israelachvili, *Intermolecular and Surface Forces* (Academic Press, San Diego, 1992), 2nd ed.
[23] L. Starrs, W. Poon, D. Hibberd, and M. Robins, J. Phys. Condens. Matter **14**, 2485 (2002).